

Two hierarchically organized neural systems for object information in human visual cortex

Christina S Konen^{1,2} & Sabine Kastner¹⁻³

The primate visual system is broadly organized into two segregated processing pathways, a ventral stream for object vision and a dorsal stream for space vision. Here, evidence from functional brain imaging in humans demonstrates that object representations are not confined to the ventral pathway, but can also be found in several areas along the dorsal pathway. In both streams, areas at intermediate processing stages in extrastriate cortex (V4, V3A, MT and V7) showed object-selective but viewpoint- and size-specific responses. In contrast, higher-order areas in lateral occipital and posterior parietal cortex (LOC, IPS1 and IPS2) responded selectively to objects independent of image transformations. Contrary to the two-pathways hypothesis, our findings indicate that basic object information related to shape, size and viewpoint may be represented similarly in two parallel and hierarchically organized neural systems in the ventral and dorsal visual pathways.

The primate visual system is broadly organized into two segregated pathways, a ventral stream that includes areas of temporal cortex and is involved in object vision and a dorsal stream that includes areas of posterior parietal cortex (PPC) and is involved in spatial vision and visually guided actions^{1,2}. In accordance with the two-pathways hypothesis, neuroimaging studies suggest that, in humans, objects are represented in a large swath of ventral temporal and lateral occipital cortex, referred to as the lateral occipital complex (LOC). LOC responds more strongly to pictures of objects than to their scrambled counterparts³⁻⁵ and shows a number of response properties that characterize an effective object recognition system subserving perceptual object constancy. First, LOC responds similarly to objects defined by luminance, texture, motion and other cues, thus representing objects independent of the precise physical cues that define an object^{6,7}. Second, LOC represents objects invariant of changing external viewing conditions such as viewpoint or transformations of object size^{4,8-10}. These neuroimaging studies are in agreement with earlier monkey physiological studies showing object-selective responses as well as size invariance and viewpoint invariance in neurons of inferior temporal cortex¹¹⁻¹⁴, which may be homologous to human LOC.

Although neural representations of object information have been extensively studied in the ventral pathway, little is known about them in the dorsal pathway. In monkeys, object-related activity has been typically found in the context of visually guided actions such as grasping, specifically in the anterior intraparietal area (AIP)^{15,16}. Occasionally, object-related activity has been reported under passive viewing conditions and, thus, independent of action planning^{4,10,17-21}. However, the functional role of this object-related activity in dorsal-stream areas is poorly understood and has been attributed, in humans,

to attentional modulation^{4,7}. Here, we used functional magnetic resonance imaging (fMRI) adaptation (fMR-A) to probe object-selective response properties of human dorsal-stream areas in relation to those of ventral-stream areas.

fMR-A has become a tool frequently used to go beyond the spatial-resolution limitations of conventional fMRI in order to probe neural selectivity in specific cortical areas⁴. fMR-A is a robust phenomenon in which repeated presentations of the same visual stimulus leads to gradual response reductions as a function of repetition frequency. Using parametric fMR-A designs, we investigated neural representations of different types of object stimuli (two-dimensional (2D) and three-dimensional (3D) objects; line drawings of objects and tools) as well as size invariance and viewpoint invariance in topographically defined areas of visual, parietal and frontal cortex. We found object-selective responses in several areas of ventral and dorsal extrastriate cortex and in areas of the PPC (IPS1, IPS2). Object-related responses in extrastriate areas at intermediate processing stages—V4 in the ventral stream and V3A, MT and V7 in the dorsal stream—depended on viewpoint and size, whereas that in areas at advanced processing stages—LOC in the ventral stream and IPS1 and IPS2 in the dorsal stream—showed size- and viewpoint-invariant response properties. Our findings suggest the existence of two parallel hierarchical neural systems for object information in the human ventral and dorsal pathways.

RESULTS

Design and definitions of areas

We investigated neural representations related to different types of object stimuli in visual, parietal and frontal cortex using fMR-A protocols ($N = 6$). In a parametric design, we tested four levels of

¹Department of Psychology, ²Center for the Study of Brain, Mind, and Behavior and ³Princeton Neuroscience Institute, Green Hall, Princeton University, Princeton, New Jersey 08540, USA. Correspondence should be addressed to C.S.K. (ckonen@princeton.edu).

Received 1 November 2007; accepted 13 December 2007; published online 13 January 2008; doi:10.1038/nn2036

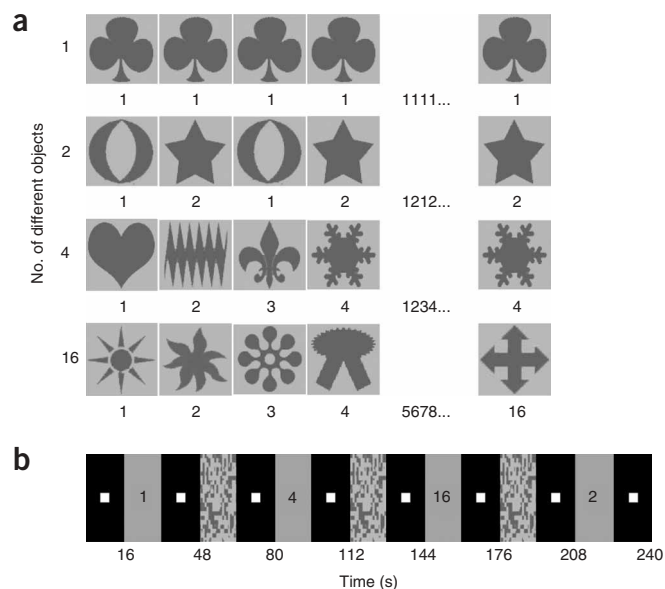


Figure 1 Experimental design. **(a)** Example of the four conditions used in the parametric fMR-A design from the 2D-object experiment. Each row represents one presentation condition. The number of identical object stimuli presented in a given condition is indicated on the left. In condition 1, the same object was presented 16 times. In condition 2, two different objects were presented eight times each. In condition 4, four object stimuli were presented four times each. Condition 16, in which 16 different stimuli were presented once each, served as a baseline to which all other conditions were compared. **(b)** Example sequence of epochs. Epochs of object presentations (conditions 1, 2, 4 and 16) were alternated with epochs of presentations of scrambled object stimuli interleaved with blank periods during which only a fixation point was present on the screen. Each epoch lasted for 16 s.

Two- and three-dimensional objects

In the first series of experiments, we probed 2D and 3D objects (**Supplementary Fig. 3a,b** online), which have been shown to evoke shape-selective responses in the lateral intraparietal area (LIP) in monkey physiological experiments^{17,19}. Time courses of fMRI signals and mean signal changes evoked by 2D objects are shown for areas V1, LOC and IPS1–4 in **Figures 2** and **3a**, respectively. Adaptation effects were defined on the basis of two criteria: a main effect of presentation condition as determined by a one-way repeated-measures analysis of variance (ANOVA) and a significant response difference between the maximally adapted and unadapted conditions ($\Delta_{1,16}$).

In agreement with previous reports^{6,20}, adaptation effects were found with 2D and 3D objects in V4 and LOC of the ventral pathway (main effect of fMR-A, $P < 0.01$; $\Delta_{1,16}$, $P < 0.01$; **Figs. 2** and **3** and **Supplementary Fig. 4a,b** online). For example, in LOC, the unadapted stimuli evoked twice as much activity as the identical stimuli, indicating a strong adaptation effect. In both areas and for both object types, epochs during which two and four images were repeated showed a gradual reduction of signal magnitude relative to the unadapted condition, reflecting the parametric modulation of the experimental protocol (**Figs. 2** and **3a,b** and **Supplementary Fig. 4a,b**).

Notably, significant adaptation effects induced by 2D and 3D objects were also found in V3A, MT, V7, IPS1 and IPS2 of the dorsal pathway (main effect of fMR-A, $P < 0.05$; $\Delta_{1,16}$, $P < 0.05$; **Figs. 2** and **3a,b** and **Supplementary Fig. 4a,b**). As in the ventral pathway, these areas

object adaptation defined by the repetition frequency of identical object stimuli⁴. In the maximal adaptation condition, the same object was presented 16 times. In intermediate adaptation conditions, two objects were presented eight times each, or four objects were presented four times each. In the unadapted condition, 16 different objects were presented once (**Fig. 1a**). Presentations of object stimuli alternated with presentations of their scrambled counterparts, interleaved with blank periods (**Fig. 1b**). Visual stimuli were presented in the center of the screen while subjects maintained fixation at a central cross and passively viewed them.

Based on previous findings^{4,5,7}, we predicted that, if a given area has object selectivity, increased repetition frequency of an object will lead to gradual response reductions, or adaptation effects, with strongest response differences between the maximally adapted and the unadapted conditions. In contrast, a region that does not show object selectivity will respond similarly in all conditions and thus show no adaptation effects.

We were particularly interested in comparing object-related activity in areas along the ventral and dorsal pathways, which were defined on the basis of topographic and functional criteria. The borders of visual areas V1, V2, V3, V4, V3A and V7 were delineated based on retinotopic mapping^{22–24}. LOC was defined by comparing epochs of intact and scrambled object presentations^{3–5,7}. Human MT was defined as the area located near the inferior temporal sulcus responding significantly stronger to presentations of moving versus stationary dots²⁵. A memory-guided saccade task served to identify topographically organized areas in parietal and frontal cortex (**Supplementary Fig. 1** online)^{24,26–28}. The intraparietal sulcus (IPS) yielded four topographically organized areas (**Supplementary Fig. 2** and **Supplementary Table 1** online). Two areas were located in the posterior part of the IPS (IPS1, IPS2)^{24,27,29}, the other two areas were located in the anterior/lateral branch of the IPS (IPS3, IPS4)²⁴. Finally, in frontal cortex, a topographic map was found in the superior branch of the precentral sulcus and caudalmost part of the superior frontal sulcus²⁸, consistent with the location of the human frontal eye field (FEF). We assigned activated voxels to these regions of interest (ROIs) based on the comparison between intact object presentations versus blank periods ($P < 0.01$). Each type of object stimuli evoked significant activation in all of the aforementioned ROIs (main effect of visual stimulation, $P < 0.05$).

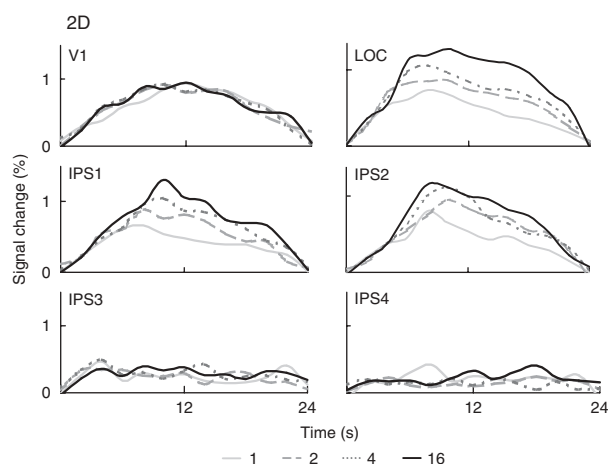


Figure 2 Time courses of fMRI signals in V1, LOC and IPS1–4 from the 2D-object experiment. Group analysis ($N = 6$). The different presentation conditions are indicated by different shades (light gray, adapted condition; intermediate grays, intermediate conditions; black, unadapted condition), and also by the key, with the numbers corresponding to the four conditions specified in **Figure 1**.

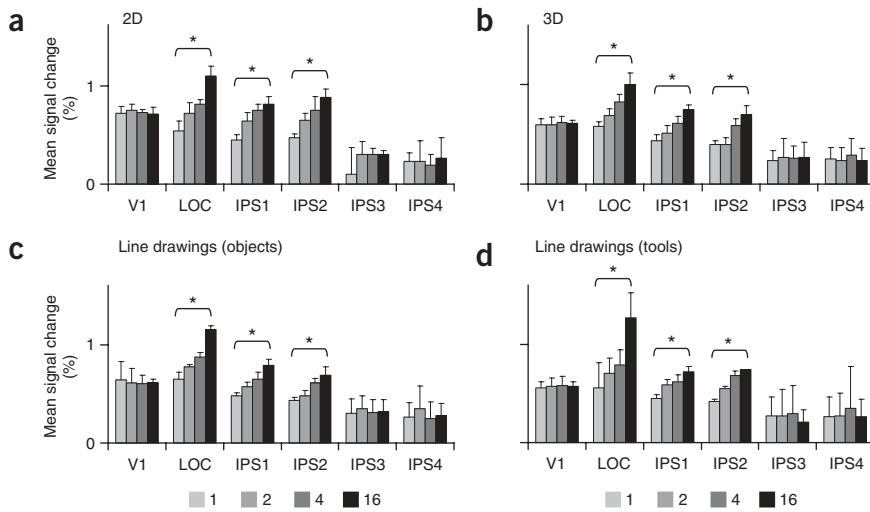


Figure 3 Mean signal changes in V1, LOC and IPS1–4. (**a–d**) Results from the experiments probing 2D objects (**a**), 3D objects (**b**), line drawings of objects (**c**) and line drawings of tools (**d**). Mean fMRI signals were averaged across subjects ($N = 6$) for each area and each of the four conditions. For each subject, mean signal change was defined as the average of the six peak intensities of the fMRI signal obtained during object presentations. *Significant differences between the adapted (1) and the unadapted (16) condition, $P < 0.05$.

showed gradual response reductions with increasing repetition frequency for 2D and 3D objects. The response profiles of IPS1 and IPS2 in the posterior branch of the IPS differed from those of IPS3 and IPS4 in the anterior/lateral branch of the IPS. Both anterior IPS areas and FEF were only weakly activated by these objects and showed similar levels of activity in response to the different presentation conditions, and thus they showed a lack of adaptation effects (main effect of fMR-A, $P > 0.05$; **Figs. 2** and **3a,b** and **Supplementary Fig. 4a,b**). Similarly, early visual areas V1, V2 and V3 showed no adaptation effects (main effect of fMR-A, $P > 0.05$; **Figs. 2** and **3a,b** and **Supplementary Fig. 4a,b**).

We quantified the adaptation effects by an adaptation index (AI), which estimates the response difference between the maximally adapted and the unadapted conditions and permits a comparison of the relative strength of the adaptation effects across areas and types of

object stimuli. Positive index values indicate stronger responses to unadapted than to adapted conditions, negative values indicate the opposite, and values around zero indicate the absence of adaptation effects. This analysis confirmed the lack of adaptation effects in V1, V2, V3, IPS3, IPS4 and FEF, with AIs not different from zero for both object types ($P > 0.05$; **Fig. 4a**). In the ventral pathway, the AIs were found to be significantly different from zero in V4 and LOC ($P < 0.01$; **Fig. 4a**), with stronger adaptation effects in LOC than in V4 ($P < 0.01$). In the dorsal pathway, AIs were significantly different from zero in V3A, MT, V7, IPS1 and IPS2 ($P < 0.01$; **Fig. 4a**). The AIs in IPS1 and IPS2 were similar to each other ($P > 0.05$), but they were significantly greater than those in the other dorsal areas ($P < 0.05$). Area V7 showed weaker effects than the two posterior IPS areas ($P < 0.05$) but stronger effects than V3A and MT ($P < 0.05$). A direct comparison between the two pathways revealed that, of areas showing adaptation effects in response to 2D and 3D objects, V3A and MT showed overall the

Line drawings of semantically meaningful objects and tools

weakest effects ($P < 0.05$), V4 and V7 showed intermediate effects ($P < 0.05$), and LOC, IPS1 and IPS2 showed the strongest adaptation effects ($P < 0.01$). The index values in LOC were significantly greater than those in IPS1 and IPS2 for 2D objects ($P < 0.01$) but similar across these areas for 3D objects ($P > 0.05$).

In the second series of experiments, we asked whether object-selective responses in ventral and dorsal pathways generalized from simple and complex shape stimuli to semantically meaningful object stimuli by probing line drawings of objects and tools (**Supplementary Fig. 3c,d**). The latter stimulus type was of particular interest because tools may be automatically linked with actions that are executed during their usage and have been shown to evoke activations in human PPC^{30,31}. Since neural responses in monkey AIP, an area located in the anterior branch

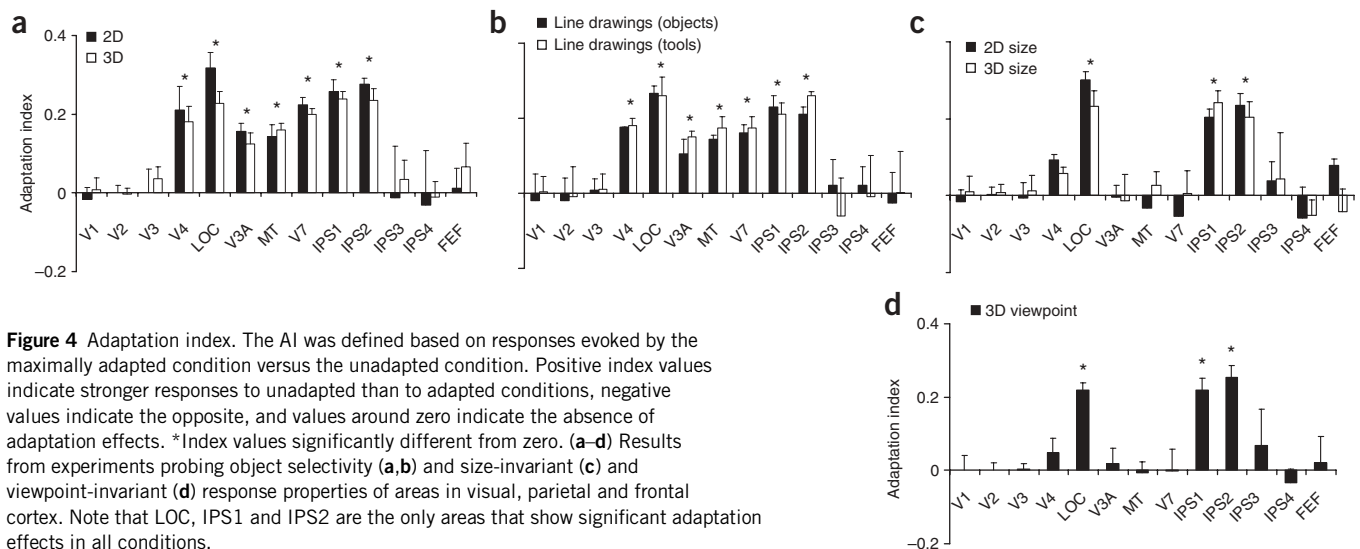


Figure 4 Adaptation index. The AI was defined based on responses evoked by the maximally adapted condition versus the unadapted condition. Positive index values indicate stronger responses to unadapted than to adapted conditions, negative values indicate the opposite, and values around zero indicate the absence of adaptation effects. *Index values significantly different from zero. (**a–d**) Results from experiments probing object selectivity (**a,b**) and size-invariant (**c**) and viewpoint-invariant (**d**) response properties of areas in visual, parietal and frontal cortex. Note that LOC, IPS1 and IPS2 are the only areas that show significant adaptation effects in all conditions.

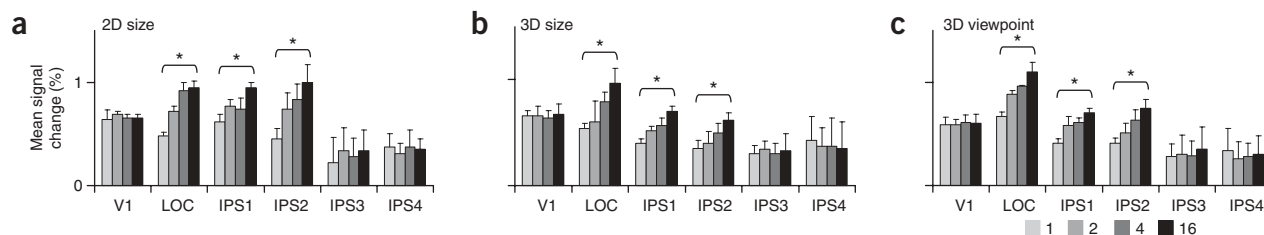


Figure 5 Mean signal changes in V1, LOC and IPS1–4. (a–c) Results from the experiments probing size-invariant (a,b) and viewpoint-invariant (c) response properties. Mean fMRI signals, defined as in **Figure 3**, were averaged across subjects ($N = 6$) for each area and for each presentation condition. *Significant differences between the adapted (1) and the unadapted (16) condition, $P < 0.05$.

of the IPS, are specifically associated with graspable but not with nongraspable objects^{15,32}, we hypothesized that IPS3 and/or IPS4 in the anterior/lateral branch of the IPS in humans might be responsive to this particular category of objects.

Both types of object stimuli yielded similar results across all areas ($P > 0.05$) and thus will be described together. In the ventral pathway, as shown in previous studies^{7,33}, V4 and LOC showed graded response reductions depending on the number of repeated line drawings of objects and tools as compared to the unadapted condition (main effect of fMR-A, $P < 0.001$; $\Delta_{1,16}$, $P < 0.001$; **Fig. 3c,d** and **Supplementary Fig. 4c,d**). In the dorsal pathway, V3A, MT, V7, IPS1 and IPS2 showed adaptation effects (main effect of fMR-A, $P < 0.05$; $\Delta_{1,16}$, $P < 0.05$; **Fig. 3c,d** and **Supplementary Fig. 4c,d**). Adaptation effects were lacking in early visual cortex and FEF (main effect of fMR-A, $P > 0.05$; **Fig. 3c,d**; **Supplementary Fig. 4c,d**). Contrary to our hypothesis, neither IPS3 nor IPS4 in the anterior/lateral IPS showed response differences between the adapted and unadapted conditions (main effect of fMR-A, $P > 0.05$; **Fig. 3c,d**). We note that such negative finding does not permit firm conclusions regarding the role of areas in anterior/lateral IPS in object-guided action. For example, it is possible that the impoverished tool images used in our stimulus set were not suitable for evoking grasping-related activations. Therefore, our findings are not necessarily in conflict with previous studies demonstrating tool-related activations in human PPC^{30,31}. Future studies using more realistic 3D tools are needed to address this issue further.

The AIs for line drawings of objects and tools are shown in **Figure 4b**. In ventral extrastriate cortex, LOC showed significantly stronger adaptation effects than V4 ($P < 0.01$). In the dorsal pathway, V3A showed smaller adaptation effects than MT and V7 ($P < 0.05$). IPS1 and IPS2 showed significantly stronger adaptation effects than V7 ($P < 0.05$). Notably, line drawings of tools elicited stronger adaptation in IPS2 than in IPS1 ($P < 0.05$), whereas line drawings of objects induced similar adaptation effects in IPS1 and IPS2 ($P > 0.05$). A direct comparison between the two pathways revealed that, of areas showing adaptation effects in response to line drawings of objects and tools, V3A showed overall the weakest adaptation effects ($P < 0.05$), V4, MT and V7 showed intermediate effects ($P < 0.05$), and LOC, IPS1 and IPS2 showed the strongest effects ($P < 0.01$).

Taken together, object-selective responses to geometric 2D and 3D objects and to line drawings of meaningful objects and tools were found not only in areas along the ventral pathway, as previously reported^{3,4,7,34}, but also in several areas along the dorsal pathway, including V3A, MT, V7, IPS1 and IPS2. The object selectivity of these areas seemed to generalize across several classes of objects. The comparison of adaptation effects induced by geometric objects and line drawings yielded no main difference between these experiments ($P > 0.05$). Importantly, LOC and the posterior IPS consistently

showed the highest AIs and hence the strongest adaptation effects as compared to other areas of the ventral and dorsal pathways. These adaptation effects, however, might simply reflect adaptation to low-level features of the object stimuli. We explored this possibility further in a third series of experiments.

Size and viewpoint invariance

In the ventral pathway, LOC responds invariantly to object size and viewpoint, indicating a high-level representation necessary for perceptual object constancy rather than a low-level representation of object features^{4,8,34}. To dissociate high-level from low-level object representations in areas along the ventral and dorsal pathways, we investigated the invariant properties for the size and viewpoint of 2D and 3D objects and compared them across the two pathways. We hypothesized that neural populations tuned to low-level features of an object would show a release from the fMR-A effects when different sizes or viewpoints of the same object were presented. However, neural populations having size- or viewpoint-invariant response properties would show fMR-A effects under such conditions. For the invariance studies, the adapted condition consisted of the repeated presentations of identical objects in 16 different sizes or viewpoints (**Supplementary Fig. 3e–g**), and the unadapted condition consisted of 16 different objects. Accordingly, the intermediate conditions consisted of two or four different objects presented in different sizes and viewpoints, respectively. The amount of physical stimulus change between the adapted and unadapted conditions was matched (see Methods for dissimilarity index).

Since the response profiles evoked in ventral and dorsal areas by 2D and 3D objects presented in different sizes and viewpoints were qualitatively similar, we will describe the results together. In the ventral pathway, V4 and LOC showed a dissociation of response patterns. When identical stimuli differing in size and viewpoint were presented, V4 showed a recovery from adaptation, consistent with the idea that the previously observed adaptation effects seen with identical stimuli having the same size or viewpoint were due to adaptation to low-level features (main effect of fMR-A, $P > 0.05$; **Supplementary Fig. 4e–g**). In accordance with previous studies^{4,8,34}, LOC was maximally activated by images of 16 different objects and was adapted by repeated presentations of identical objects in 16 different sizes or viewpoints, indicating size- and viewpoint-invariant coding of object information (main effect of fMR-A, $P < 0.001$; $\Delta_{1,16}$, $P < 0.001$; **Fig. 5**). A similar dissociation occurred in dorsal areas, where V3A, MT and V7 all no longer showed adaptation when probed with identical stimuli differing in size or viewpoint (main effect of fMR-A, $P > 0.05$; **Supplementary Fig. 4e–g**), whereas IPS1 and IPS2 showed significant adaptation, thus showing size- and viewpoint-invariant properties similarly to LOC (main effect of fMR-A, $P < 0.01$; $\Delta_{1,16}$, $P < 0.01$; **Fig. 5**). The AIs confirmed that LOC, IPS1 and IPS2 were the only areas

showing significant adaptation effects in the invariance experiments ($P < 0.01$; **Fig. 4c,d**). As in our study under identical viewing conditions, 2D objects elicited stronger adaptation effects in LOC than in IPS1 and IPS2 ($P < 0.001$), but 3D objects induced similar adaptation effects in LOC and the posterior IPS ($P > 0.05$).

Taken together, the invariance studies showed that adaptation in LOC, IPS1 and IPS2 remained under different viewing conditions of an object, indicating the representation of global rather than local aspects of object information at advanced processing stages of both pathways. In contrast, activity in intermediate areas of the visual hierarchy no longer showed adaptation, suggesting the processing of low-level aspects of object information.

Attentional control experiment

Object-related activations in areas of the dorsal pathway have previously been attributed to attentional modulation of visually evoked activity, rather than to the representation of object information^{7,35}. Therefore, it may be argued that the differences in activation evoked during adapted and unadapted conditions found in our studies were confounded by attention, because subjects may have paid less attention to repeatedly presented objects and more attention to sequences of different stimuli. To exclude this possibility, we repeated two of our studies (2D objects, 2D objects in different sizes) while top-down attentional effects were controlled. In these studies, subjects were instructed to track the number of luminance changes at fixation. In one series of control studies, they executed a motor response: subjects pressed a button whenever they detected a luminance change at fixation. Because the higher-order areas of the dorsal pathway are associated with sensory-motor transformation and a motor response may therefore influence the activity evoked in dorsal areas, we ran a second series of studies in which subjects reported the number of luminance changes at the end of each scan and thus did not execute a motor response. We tested only the maximally adapted and unadapted conditions in these control studies.

We assessed the efficacy of the luminance detection task by analyzing performance in the fixation task as a function of presentation condition. For 2D objects, accuracy for adapted and unadapted conditions was $81 \pm 6\%$ and $80 \pm 7\%$, respectively, and the average reaction times were 478 ± 97 ms and 459 ± 123 ms, respectively; the differences between these values were not significant for either measure ($P > 0.05$; **Supplementary Fig. 5** online). For 2D objects in different sizes, accuracy as well as average reaction times for adapted and unadapted conditions were similar ($79 \pm 7\%$ and $82 \pm 4\%$, respectively; $P > 0.05$; 462 ± 92 ms and 472 ± 100 ms, respectively; $P > 0.05$; **Supplementary Fig. 5**). Thus, the reaction times together with the accuracy suggest that attention was evenly distributed across the adapted and unadapted conditions.

The fMRI results showed that, relative to the passive viewing condition, activity significantly decreased when subjects performed the fixation task. Such attentional suppression effects were significant in areas V1, V2, V4, LOC, MT, V7, IPS1 and IPS2 (main effect of attention, $P < 0.05$). For 2D objects, the attentional suppression effects ranged between 0.09% and 0.55% (in V1 and V4, respectively). For 2D objects in different sizes, the attentional suppression effects ranged between 0.11% and 0.51% (V1 and V4, respectively). The signal decrease during the performance of the fixation task was similar for 2D objects and 2D objects in different sizes ($P > 0.05$). However, there was no interaction effect between attention and adaptation effects ($P > 0.05$). The adaptation effects obtained with the luminance detection task were not different from those found with passive fixation ($P > 0.05$; **Supplementary Fig. 6** online). The adaptation effects induced by 2D objects in ventral areas V4 and LOC and dorsal areas

V3A, MT, V7, IPS1 and IPS2 were replicated under both of the active task conditions ($P < 0.05$; **Supplementary Fig. 6a**). Similarly, the dissociation of adaptation effects found with the size-invariance studies was replicated in areas along the ventral and dorsal pathways ($P < 0.01$; **Supplementary Fig. 6b**). Taken together, the attentional control studies showed that the object-selective response properties of ventral and dorsal areas were little affected when attention was engaged at fixation and thus drawn away from the object stimuli, indicating that adaptation effects in the dorsal pathway, and in particular in PPC, could not be easily attributed to attentional modulation.

DISCUSSION

Here, we demonstrate object-selective responses in areas along the ventral and dorsal pathways by using parametric fMR-A designs and an ROI approach that identified topographically organized areas in human visual, parietal and frontal cortex. These object-related neural representations seemed to generalize across several types of stimuli, including 2D and 3D objects and line drawings of objects and tools. In both pathways, areas at intermediate stages of cortical processing, such as V4, V3A, MT and V7, showed size- and viewpoint-specific responses, whereas high-level areas in ventral visual cortex such as LOC and in PPC such as IPS1 and IPS2 responded invariantly to these image transformations. We found no object-selective responses in the anterior/lateral IPS (IPS3 and IPS4), implying functional differences across topographically organized areas of PPC.

We considered the possibility that object adaptation effects found in the dorsal pathway might have been confounded by differences in the allocation of attentional resources across the different presentation conditions if subjects paid more attention to epochs containing different objects than to those containing identical objects^{7,35}. Neural activity in the PPC in particular is known to be strongly modulated by visual attention^{36–38}. For several reasons, this interpretation is not likely. First, our attentional control studies showed that adaptation effects in ventral and dorsal areas were not significantly affected when attention was engaged at fixation and thus drawn away from the object stimuli. Second, the dissociation of adaptation effects between intermediate areas and higher-order areas observed in the invariance studies is incompatible with an attentional modulation account. Areas such as V4 and MT are known to be considerably modulated by attention³⁹, but they did not show adaptation effects in these experiments. Likewise, adaptation effects differed among the various topographically organized areas of parietal and frontal cortex, which are all part of the general attentional network (S.M. Szczepanski & S.K., unpublished observations), with adaptation effects being seen in IPS1 and IPS2 but not in IPS3, IPS4 and FEF, which is not compatible with general attentional effects as the source of the observed fMR-A effects. Taken together, the attentional control studies and the specific response patterns found across areas and conditions rule out the possibility that attentional modulation confounded our studies to any great extent.

Our findings confirm and extend previous studies on object-selective representations in the ventral pathway. In humans, object selectivity in LOC has been reported for several types of object stimuli, such as photographs, line drawings and 3D objects^{3,4,7,34}. It has also been shown that LOC responds invariantly to image transformations such as size, position and viewpoint^{4,8,10,34}, and thus this area may be part of a recognition system that subserves perceptual object constancy⁴⁰. In contrast, we found that V4 responded selectively to a variety of object stimuli, but these responses depended on the object size and viewpoint. These findings indicate the importance of human V4 in the analysis of object form and imply a close functional similarity between human and monkey V4, which contains neurons responding to a variety of simple

and complex object features^{41–43}. The dissociation of neural responses with respect to viewpoint and size between V4 and LOC is in agreement with studies in monkeys showing that neurons at successive stages of the ventral pathway encode progressively more complex attributes of an object, with neurons in inferior temporal cortex showing response properties invariant to image transformations^{10–12,14}. Thus, our findings provide converging evidence to support the notion of a hierarchical organization of neural representations related to object information in the ventral pathway of primates⁴⁰.

Notably, we found a similar hierarchically organized neural system of object representations in the dorsal pathway. As in the ventral system, object-selective, size-dependent and viewpoint-dependent responses were present in areas at intermediate processing stages, such as V3A, MT and V7, whereas higher-order areas of PPC showed object-selective responses invariant to image transformations. Thus, the dorsal system of object representations seemed to parallel the well-known ventral system in terms of basic response properties. There are a number of important characteristics of object representations in the dorsal pathway. First, the object responses were found under passive viewing conditions, or even when attention was drawn away from the stimuli, and were thus independent of a behavioral context that required action planning. Second, with the exception of that evoked by 2D shapes, the dorsal object-related activity appeared indistinguishable from that in the ventral stream. And third, the object-related activity in PPC was not specific to changes of viewpoint and size but rather were generalized across changing viewing conditions.

These findings corroborate and extend previous studies of shape-selective responses in LIP neurons of monkey PPC, which were elicited by 2D objects under passive viewing conditions¹⁷. In the monkey, LIP neurons showed weaker selectivity to 2D objects than inferior temporal cortex neurons¹⁹. Notably, we also found weaker adaptation effects induced by 2D objects in IPS1 and IPS2 than in LOC. This finding may be interpreted to reflect weaker object selectivity in PPC than in LOC. However, no differences in the strength of object adaptation effects were found in posterior IPS and LOC for 3D objects and for line drawings of objects and tools, which have not been investigated in nonhuman primates. In addition, both monkey LIP and human posterior IPS are engaged during saccadic eye movements, spatial attention and working memory tasks^{17,27,29,38,44}. These findings together with the present results may indicate that IPS1 and IPS2 are possible homologs of monkey LIP.

Studies from humans with damage to the ventral pathway indicate that the dorsal pathway mediates the control of actions directed at graspable objects, which are subserved by neural mechanisms distinct from those mediating the perception of those objects⁹. These findings are corroborated by monkey physiological and human neuroimaging studies. In monkeys, object-related responses in PPC have typically been reported in association with action planning, particularly in tasks that require the execution of grasping movements³². For example, area AIP contains both visual- and motor-related neurons for the neural coding of finger shaping in monkeys trained to grasp objects^{15,16}. In humans, activations in the anterior IPS have been found while subjects viewed graspable objects such as tools, which appear to be automatically linked to actions that are executed during their usage, but not while they viewed nongraspable objects^{30,31}. It has been argued that LIP serves as a relay conveying object information to AIP (ref. 45). Thus, it is conceivable that IPS1 and IPS2 have similar roles in relaying object information from intermediate processing areas to regions in the anterior IPS in the human brain. However, several of our observations indicate that object-related activity in the dorsal pathway may serve broader functional purposes in perception and cognition.

First, we found representations for a variety of different object stimuli in the human PPC when action planning was not involved and even when attention was drawn away from the stimuli. Notably, most of our stimuli were not associated with actions, and yet they still activated the posterior PPC strongly. These findings are in agreement with previous monkey fMRI studies that were performed in anesthetized animals and showed activations evoked by 3D objects in both visual pathways¹⁸. Together, these findings provide strong evidence that object information is represented in the dorsal pathway independent of action planning. Second, the dorsal system for object information showed very similar response patterns to those in the ventral system. Most notably, the top stages of both systems showed generalized responses across changes in stimulus appearance such as size and viewpoint. Although it is widely agreed that a successful object recognition system requires generalization across changing viewing conditions⁴⁰, one would predict that a system that uses object information for the control of skilled actions would preserve the specificity of object appearance with regard to shape, size and orientation⁴⁶. For example, the same object presented from different viewpoints would require different hand postures during grasping⁹. Our finding of object-related activity that generalized across image transformations therefore does not support a view that object information in the dorsal pathway is used merely for sensory-motor transformations in visually guided behavior.

The classical view of the two-pathway hypothesis suggests the existence of two anatomically distinct and functionally specialized pathways: a ventral stream for object vision and a dorsal stream for spatial vision¹. At some level of neural processing, information about the identity and location of an object that is represented in the segregated pathways must be integrated. This integration could be implemented in several ways, not mutually exclusive. One possibility is that the integration of object and location information occurs in a common higher-order area that both streams project to, such as prefrontal cortex, as suggested by physiological studies in monkeys⁴⁷. Another possibility is that there is parallel encoding of object information in the two pathways, as suggested by the present study. Areas in the PPC have a detailed spatial map of the visual field in addition to their object-selective response properties. Therefore, these areas may be ideally suited for a functional role as integrators of spatial and object information. In summary, our findings imply the existence of two parallel and hierarchically organized neural systems for object representation along the ventral and dorsal visual pathways. The functional role of the dorsal system in action, perception and cognition remains to be explored.

METHODS

Subjects, visual stimuli and experimental design. Six healthy subjects (20–36 years old, three of them men, normal or corrected-to-normal visual acuity) gave informed written consent for participation in the study, which was approved by the Institutional Review Panel of Princeton University. Each subject participated in five sessions to perform the fMR-A studies and three sessions for the localization of areas in visual, parietal and frontal cortex (see **Supplementary Methods** online for details).

We conducted seven fMR-A studies. Four studies investigated adaptation effects of different object categories: 2D and 3D objects and line drawings of meaningful objects and tools (**Fig. 1** and **Supplementary Fig. 3a–d**). To test size and viewpoint invariance, three studies used different sizes of 2D and 3D objects and different viewpoints of 3D objects (**Fig. 1** and **Supplementary Fig. 3e–g**).

For each fMR-A study, 96 grayscale images of 2D objects (11.5 cd m⁻²), 3D objects (12.6 cd m⁻²), line drawings of meaningful objects (14.6 cd m⁻²), or line drawings of tools (14.6 cd m⁻²) were used (**Supplementary Figs. 3a–d**). The

same set of objects was scrambled into blocks of 25×25 pixels. The stimuli subtended approximately $18^\circ \times 18^\circ$ of visual angle centered over a fixation point on a gray background (23.4 cd m^{-2}). 2D and 3D objects were generated with MATLAB software (MathWorks); line drawings of objects and tools were chosen from the Word ClipArt Gallery (Microsoft). For the size-invariance studies, the sets of 2D and 3D objects were changed in size, resulting in 16 different sizes of each object over a range of $6.75^\circ \times 6.75^\circ$ to $18^\circ \times 18^\circ$ (Supplementary Fig. 3e–f). For the viewpoint-invariance studies, the 3D objects were rotated around the y axis to create rotations to various angles, resulting in 16 different viewpoints of each object covering a range of $\pm 75^\circ$ (Supplementary Fig. 3g).

A dissimilarity index⁴ d_{jk} was computed to estimate the physical stimulus change in conditions with identical object images under different viewing conditions (adapted condition) and conditions with different object images (unadapted condition), as used in the invariance studies. This index is a quantitative measure of the mean pixel-wise changes caused by identical objects under different viewing conditions and different objects presented in a given epoch.

$$d_{jk} = \frac{1}{n} \sqrt{\sum_{x=1}^n [l_j(x) - l_k(x)]^2} \quad [j, k = 1 \dots p]$$

n is the number of pixels in an object image, $l_j(x)$ is the bitmap gray level value of the pixel in location x of image l_j , and p is the number of images in an epoch. The greater the dissimilarity index, the greater is the physical dissimilarity between the object images. It is important to establish a close match between the adapted and unadapted conditions to exclude the possibility that differential response profiles evoked by these conditions are attributable to physical dissimilarity. The indexed changes for identical objects in different sizes and viewpoints were 6.3 ± 2.5 and 6.1 ± 1.9 , respectively. The indexed change for different objects was 4.9 ± 1.6 . The dissimilarity index was not significantly different across conditions ($P > 0.05$).

Each fMR-A study consisted of six scans, each of which contained four epochs of intact object presentations and three epochs of scrambled object presentations. Each epoch lasted for 16 s and was alternated with equally long blank periods (Fig. 1b). In each epoch, 16 intact or scrambled objects were presented for 750 ms each, interposed with 250-ms blank periods. Each scan started and ended with a blank period of 16 s. A central fixation point (0.5°) was presented during the whole scan and subjects were instructed to maintain fixation. To control for attentional effects, subjects were retested in two experiments (2D objects and 2D objects in different sizes) during which they were asked to track the number of luminance changes at fixation. The control studies comprised only the maximally adapted and unadapted conditions, not the intermediate adaptation conditions. In one series of attentional control experiments, subjects pressed a button whenever they detected a luminance change. In the other series of experiments, subjects reported the number of luminance changes at the end of each scan. The luminance changes occurred on average every 2.6 s. Before scanning, each subject was trained in behavioral sessions outside the scanner to maintain fixation for several minutes while eye movements were monitored with an infrared eye tracker (Applied Science Laboratories).

The fMR-A protocols varied object adaptation parametrically by investigating four levels of object adaptation that were distinguished by the number of different objects presented in a given epoch: the same object presented 16 times, two different objects presented eight times each, four different objects presented four times each and 16 different objects presented once (Fig. 1a). The order of conditions was randomized across scans (for an example sequence, see Fig. 1b). For the size- and viewpoint-invariance studies, the adapted condition consisted of the repeated presentations of identical objects in 16 different sizes or viewpoints, while the unadapted condition consisted of 16 different objects and the intermediate conditions consisted of two or four different objects presented in different sizes or viewpoints.

Visual display. The stimuli were generated on a Macintosh G4 computer (Apple) using MATLAB and Psychophysics Toolbox functions^{48,49}. Stimuli were projected from a PowerLite 7250 liquid crystal display projector (Epson) outside the scanner room onto a translucent screen located at the end of the

scanner bore. Subjects viewed the screen at a total path length of 60 cm through a mirror attached to the head coil. The screen subtended 30° of visual angle in the horizontal dimension and 26° in the vertical dimension. A trigger pulse from the scanner synchronized the onset of stimulus presentation to the beginning of the image acquisition.

Data acquisition and analysis. Data were acquired with a 3-T head scanner (Allegra, Siemens) using a standard head coil. An anatomical scan (MPRAGE sequence, TR = 2.5 s, TE = 4.3 ms, flip angle = 8° , 256×256 matrix, 1-mm³ resolution) was acquired in each session to facilitate cortical surface alignments. For the fMR-A experiments, functional images were taken with a gradient echo, echoplanar sequence (TR = 2 s, TE = 30 ms, flip angle = 90°). Thirty-four axial slices (slice thickness 3 mm, gap 0 mm, voxel size $3 \times 3 \times 3 \text{ mm}^3$) covering the whole brain were acquired in six series of 240 volumes for each experiment.

Data were analyzed using AFNI (<http://afni.nimh.nih.gov/afni>), FRESURFER (<http://surfer.nmr.mgh.harvard.edu>) and SUMA (<http://afni.nimh.nih.gov/afni/suma>). For the fMR-A studies, the functional images were motion-corrected to the image acquired closest to the anatomical scan and normalized to percentage signal change by dividing the time series by its mean intensity. Square-wave functions matching the time course of the experimental design were convolved with a gamma-variate function and used as regressors of interest in a multiple regression model in the framework of the general linear model⁵⁰. In the model, we also included regressors to account for variance due to baseline shifts between time series, linear drifts within time series, and head motion.

Activated voxels resulting from the comparison between intact object and blank presentations ($P < 0.01$) were assigned to ROIs. Time series of fMRI intensities were averaged over these activated voxels within the given ROIs and normalized to the mean intensity obtained during the blank periods. All time-course analyses were performed on unsmoothed data. For each subject, the six peak intensities of the fMRI signal obtained during the object presentations were averaged, resulting in mean signal changes. The mean signal changes were then averaged across subjects to yield group data. Statistical significance was assessed with a one-way repeated-measures ANOVA followed by a multiple comparison test (t -test) on the mean signal changes of the group analysis. To quantify the adaptation effects and compare them across studies and areas, an adaptation index (AI) was computed for each area and study: $\text{AI} = (R_{\text{different}} - R_{\text{identical}}) / (R_{\text{different}} + R_{\text{identical}})$, where $R_{\text{identical}}$ is the mean fMRI signal obtained during the maximally adapted condition and $R_{\text{different}}$ the mean fMRI signal obtained during the unadapted condition. Statistical significance was assessed with a one-sample t -test against zero and a two-way repeated-measures ANOVA (area \times experiment) followed by a paired-samples t -test.

Note: Supplementary information is available on the Nature Neuroscience website.

ACKNOWLEDGMENTS

This study was supported by grants from the US National Institutes of Health (RO1 MH64043, RO1 EY017699, P50 MH-62196) to S.K. and a grant from the German Academic Exchange Service to C.S.K. We thank M. Graziano and A. Treisman for comments on an earlier draft and members of the Kastner lab for discussions and help in scanning experiments.

AUTHOR CONTRIBUTIONS

C.S.K. and S.K. designed the experiments; C.S.K. acquired and analyzed the data; C.S.K. and S.K. wrote the manuscript.

Published online at <http://www.nature.com/natureneuroscience>

Reprints and permissions information is available online at <http://npg.nature.com/reprintsandpermissions>

1. Ungerleider, L.G. & Mishkin, M. Two cortical visual systems. In *Analysis of Visual Behavior* (eds. Ingle, D.J., Goodale, M.A. & Mansfield, R.J.W.) 549–586 (MIT Press, Cambridge, Massachusetts, USA, 1982).
2. Goodale, M.A. & Milner, A.D. Separate visual pathways for perception and action. *Trends Neurosci.* **15**, 20–25 (1992).
3. Malach, R. *et al.* Object-related activity revealed by functional magnetic resonance imaging in human occipital cortex. *Proc. Natl. Acad. Sci. USA* **92**, 8135–8139 (1995).
4. Grill-Spector, K. *et al.* Differential processing of objects under various viewing conditions in the human lateral occipital complex. *Neuron* **24**, 187–203 (1999).

5. Kourtzi, Z. & Kanwisher, N. Representation of perceived object shape by the human lateral occipital complex. *Science* **293**, 1506–1509 (2001).
6. Grill-Spector, K., Kushnir, T., Edelman, S., Itzhak, Y. & Malach, R. Cue-invariant activation in object-related areas of the human occipital lobe. *Neuron* **21**, 191–202 (1998).
7. Kourtzi, Z. & Kanwisher, N. Cortical regions involved in perceiving object shape. *J. Neurosci.* **20**, 3310–3318 (2000).
8. Vuilleumier, P., Henson, R.N., Driver, J. & Dolan, R.J. Multiple levels of visual object constancy revealed by event-related fMRI of repetition priming. *Nat. Neurosci.* **5**, 491–499 (2002).
9. James, T.W., Humphrey, G.K., Gati, J.S., Menon, R.S. & Goodale, M.A. Differential effects of viewpoint on object-driven activation in dorsal and ventral streams. *Neuron* **35**, 793–801 (2002).
10. Sawamura, H., Georgieva, S., Vogels, R., Vanduffel, W. & Orban, G.A. Using functional magnetic resonance imaging to assess adaptation and size invariance of shape processing by humans and monkeys. *J. Neurosci.* **25**, 4294–4306 (2005).
11. Gross, C.G., Rocha-Miranda, C.E. & Bender, D.B. Visual properties of neurons in inferotemporal cortex of the macaque. *J. Neurophysiol.* **35**, 96–111 (1972).
12. Desimone, R., Albright, T.D., Gross, C.G. & Bruce, C. Stimulus-selective properties of inferior temporal neurons in the macaque. *J. Neurosci.* **4**, 2051–2062 (1984).
13. Logothetis, N.K. & Sheinberg, D.L. Visual object recognition. *Annu. Rev. Neurosci.* **19**, 577–621 (1996).
14. Booth, M.C. & Rolls, E.T. View-invariant representations of familiar objects by neurons in the inferior temporal visual cortex. *Cereb. Cortex* **8**, 510–523 (1998).
15. Murata, A., Gallese, V., Luppino, G., Kaseda, M. & Sakata, H. Selectivity for the shape, size, and orientation of objects for grasping in neurons of monkey parietal area AIP. *J. Neurophysiol.* **83**, 2580–2601 (2000).
16. Sakata, H. The role of the parietal cortex in grasping. *Adv. Neurol.* **93**, 121–139 (2003).
17. Sereno, A.B. & Maunsell, J.H. Shape selectivity in primate lateral intraparietal cortex. *Nature* **395**, 500–503 (1998).
18. Sereno, M.E., Trinath, T., Augath, M. & Logothetis, N.K. Three-dimensional shape representation in monkey cortex. *Neuron* **33**, 635–652 (2002).
19. Lehky, S.R. & Sereno, A.B. Comparison of shape encoding in primate dorsal and ventral visual pathways. *J. Neurophysiol.* **97**, 307–319 (2007).
20. Kourtzi, Z., Bulthoff, H.H., Erb, M. & Grodd, W. Object-selective responses in the human motion area MT/MST. *Nat. Neurosci.* **5**, 17–18 (2002).
21. Grill-Spector, K. & Malach, R. The human visual cortex. *Annu. Rev. Neurosci.* **27**, 649–677 (2004).
22. Sereno, M.I. *et al.* Borders of multiple visual areas in humans revealed by functional magnetic resonance imaging. *Science* **268**, 889–893 (1995).
23. Engel, S.A., Glover, G.H. & Wandell, B.A. Retinotopic organization in human visual cortex and the spatial precision of functional MRI. *Cereb. Cortex* **7**, 181–192 (1997).
24. Swisher, J.D., Halko, M.A., Merabet, L.B., McMains, S.A. & Somers, D.C. Visual topography of human intraparietal sulcus. *J. Neurosci.* **27**, 5326–5337 (2007).
25. Huk, A.C., Dougherty, R.F. & Heeger, D.J. Retinotopy and functional subdivision of human areas MT and MST. *J. Neurosci.* **22**, 7195–7205 (2002).
26. Sereno, M.I., Pitzalis, S. & Martinez, A. Mapping of contralateral space in retinotopic coordinates by a parietal cortical area in humans. *Science* **294**, 1350–1354 (2001).
27. Schluppeck, D., Glimcher, P.W. & Heeger, D.J. Topographic organization for delayed saccades in human posterior parietal cortex. *J. Neurophysiol.* **94**, 1372–1384 (2005).
28. Kastner, S. *et al.* Topographic maps in human frontal cortex revealed in memory-guided saccade and spatial working-memory tasks. *J. Neurophysiol.* **97**, 3494–3507 (2007).
29. Silver, M.A., Ress, D. & Heeger, D.J. Topographic maps of visual spatial attention in human parietal cortex. *J. Neurophysiol.* **94**, 1358–1371 (2005).
30. Culham, J.C., Cavina-Pratesi, C. & Singhal, A. The role of parietal cortex in visuomotor control: what have we learned from neuroimaging? *Neuropsychologia* **44**, 2668–2684 (2006).
31. Chao, L.L. & Martin, A. Representation of manipulable man-made objects in the dorsal stream. *Neuroimage* **12**, 478–484 (2000).
32. Sakata, H. *et al.* Neural coding of 3D features of objects for hand action in the parietal cortex of the monkey. *Phil. Trans. R. Soc. Lond. B* **353**, 1363–1373 (1998).
33. Kanwisher, N., Chun, M.M., McDermott, J. & Ledden, P.J. Functional imaging of human visual recognition. *Brain Res. Cogn. Brain Res.* **5**, 55–67 (1996).
34. Kourtzi, Z., Erb, M., Grodd, W. & Bulthoff, H.H. Representation of the perceived 3-D object shape in the human lateral occipital complex. *Cereb. Cortex* **13**, 911–920 (2003).
35. Grill-Spector, K. The neural basis of object perception. *Curr. Opin. Neurobiol.* **13**, 159–166 (2003).
36. Corbetta, M. Frontoparietal cortical networks for directing attention and the eye to visual locations: identical, independent, or overlapping neural systems? *Proc. Natl. Acad. Sci. USA* **95**, 831–838 (1998).
37. Kastner, S., Pinsk, M.A., De Weerd, P., Desimone, R. & Ungerleider, L.G. Increased activity in human visual cortex during directed attention in the absence of visual stimulation. *Neuron* **22**, 751–761 (1999).
38. Colby, C.L. & Goldberg, M.E. Space and attention in parietal cortex. *Annu. Rev. Neurosci.* **22**, 319–349 (1999).
39. O'Connor, D.H., Fukui, M.M., Pinsk, M.A. & Kastner, S. Attention modulates responses in the human lateral geniculate nucleus. *Nat. Neurosci.* **5**, 1203–1209 (2002).
40. Riesenhuber, M. & Poggio, T. Neural mechanisms of object recognition. *Curr. Opin. Neurobiol.* **12**, 162–168 (2002).
41. Desimone, R., Schein, S.J., Moran, J. & Ungerleider, L.G. Contour, color and shape analysis beyond the striate cortex. *Vision Res.* **25**, 441–452 (1985).
42. Gallant, J.L., Connor, C.E., Rakshit, S., Lewis, J.W. & Van Essen, D.C. Neural responses to polar, hyperbolic, and Cartesian gratings in area V4 of the macaque monkey. *J. Neurophysiol.* **76**, 2718–2739 (1996).
43. Pasupathy, A. & Connor, C.E. Population coding of shape in area V4. *Nat. Neurosci.* **5**, 1332–1338 (2002).
44. Andersen, R.A. Multimodal integration for the representation of space in the posterior parietal cortex. *Phil. Trans. R. Soc. Lond. B* **352**, 1421–1428 (1997).
45. Nakamura, H. *et al.* From three-dimensional space vision to prehensile hand movements: the lateral intraparietal area links the area V3A and the anterior intraparietal area in macaques. *J. Neurosci.* **21**, 8174–8187 (2001).
46. Craighero, L., Fadiga, L., Umiltà, C.A. & Rizzolatti, G. Evidence for visuomotor priming effect. *Neuroreport* **8**, 347–349 (1996).
47. Rao, S.C., Rainer, G. & Miller, E.K. Integration of what and where in the primate prefrontal cortex. *Science* **276**, 821–824 (1997).
48. Brainard, D.H. The Psychophysics Toolbox. *Spat Vis* **10**, 433–436 (1997).
49. Pelli, D.G. The VideoToolbox software for visual psychophysics: transforming numbers into movies. *Spat Vis* **10**, 437–442 (1997).
50. Friston, K.J., Frith, C.D., Turner, R. & Frackowiak, R.S. Characterizing evoked hemodynamics with fMRI. *Neuroimage* **2**, 157–165 (1995).